Numerical simulation of a single-screw plasticating extruder

Article *in* Polymer Engineering and Science · December 1982

DOI: 10.1002/pen.760221706

2 authors, including:

John Vlachopoulos
McMaster University
181 PUBLICATIONS **3,268** CITATIONS

Numerical Simulation of a Single-Screw Plasticating Extruder

E. E. AGUR* *and* J. VLACHOPOULOS

Department of Chemical Engineering
McMaster University
Hamilton, Ontario, Canada L8S 4L7

A fully-predictive steady-state computer model has been developed for a single-screw plasticating extruder. Included in the model are a model for solids flow in the feed hopper; a variation of the Darnell and Mol model for the solids conveying zone; a variation of Tadmor's melting model for the melting zone; an implicit finite difference solution of the mass, momentum, and energy conservation equations for the melt-conveying zone of the extruder and die; and a predictive correlation for the extrudate swell at the die exit. A temperature- and shear-rate-dependent viscosity equation is used to describe the melt-flow behavior in the model. The parameters in the viscosity equation are obtained by applying regression analysis to Instron capillary rheometer data. Given the material and rheological properties of the polymer, the screw geometry and dimensions, and the extruder operating conditions, the following are predicted: flow rate of the polymer, pressure and temperature profiles along the extruder screw channel and in the die, and extrudate swell at the die exit. The predictions have been confirmed with experimental results from a 1½ in. (38 mm) diameter, 24:1 L/D single-screw extruder with a 3/16 in. (4.76 mm) diameter cylindrical rod die. High- and low-density polyethylene resins were used.

INTRODUCTION

The development of mathematical models for single-screw plasticating extruders has been covered extensively in the literature (1-7). By far, the majority of these studies have concentrated on melt extruders or the melt-conveying section of plasticating extruders. The main reason for this is that the analysis and modeling of melt flow is far simpler than that of solids conveying and melting of the polymer. Applications for melt-fed extruders can be found in the polymer-processing industry; for example, in the homogenization and pelletization of the polymer immediately after polymerization. Most extruders used in the plastics industry, however, are plasticating extruders; that is, they are fed by polymer in solid granular form. The solid polymer granules flow by gravity in the hopper and into the screw channel, where they are compressed, conveyed down the screw channel, and then melted.

Modeling of a plasticating extruder should include the analysis of (5):

- gravitational flow behavior of particulate solids in hoppers (in particular, pressure distribution, arching, and bridging);
- stress and temperature distribution in the solids-conveying zone;
- rate of melting, mean width profile of the solid bed (solid-bed profile), and mean temperature of the melt flow into the melt pool in the melting zone;
- drag-induced pressurization and laminar mixing of the melt in both the melt-conveying zone and the melt pool in the melting zone;
- power consumption in the solids-conveying, melting, and melt-conveying zones;
- pressure flow in the die;
- surging conditions; and
- extrudate swelling at the die exit.

In more general terms, one should be able to obtain velocity, temperature, and stress profiles in both the solid and melt phases, from which all the other variables of interest could then be calculated.

It is our objective in this article, to describe a fully predictive computer model of a single-screw plasticating extruder (developed at the Department of Chemical Engineering, McMaster University) and to present the results of simulations and experimental runs on a 1½ in. (38 mm) diameter, 24:1 L/D single-screw extruder. The model, as compared to other extruder models described in the literature (1-7), is unique in that it is fully predictive and in-

*Present address: Xerox Research Centre of Canada, Mississauga, Ont. Canada L5K 2L1

cludes all the extrusion steps from the feed hopper to the swelling of the extrudate at the die exit. Given the material and rheological properties of the polymer, the screw geometry and dimensions, and the extruder operating conditions (screw speed and barrel-temperature profile), the model is used to predict:

- flow rate of the polymer;
- pressure and temperature profiles along the extruder screw channel and in the die; and
- extrudate swell at the die exit.

DESCRIPTION OF THE EXTRUDER MODEL

The computer model consists of six interdependent sections, as shown in *Fig. 1:* the feed hopper; the solids-conveying, melting, and melt-conveying zones; the die; and the swelling of the extrudate at the die exit. Each of these sections is described below.

Feed Hopper

Solid polymer pellets are fed into the extruder screw channel through the feed hopper, usually by gravity. The base pressure in the feed hopper may be determined by analyzing the pressure distribution in the solids. Walker (8) has derived relationships for the pressure distribution in both vertical and convergent bins, assuming stress equilibrum in the solid particles. *Equations 1* and 2, shown below, are used in combination to calculate the pressure at the base of a hopper with square cross-section, as illustrated in *Figure 2.*

Vertical Sections:

$$p = p_o \exp\left(-\frac{4BD^*H}{W}\right) + \frac{\rho_{bulk}gW}{4BD^*}\left[1 - \exp\left(-\frac{4BD^*H}{W}\right)\right] \quad (1)$$

where

$$B = \frac{\sin\delta \sin\kappa_o}{1 - \sin\delta\cos\kappa_o}$$

$$\kappa_o = \beta_w + \arcsin\left(\frac{\sin\beta_w}{\sin\delta}\right), \arcsin > \frac{\pi}{2}$$

$$\beta_w = \arctan(f'_w)$$

and where p and p_o are the pressures at the base and at height H in the vertical section, W the hopper width, ρ_{bulk} the bulk density of the solid polymer particles, g the gravitational acceleration, D^* the distribution factor

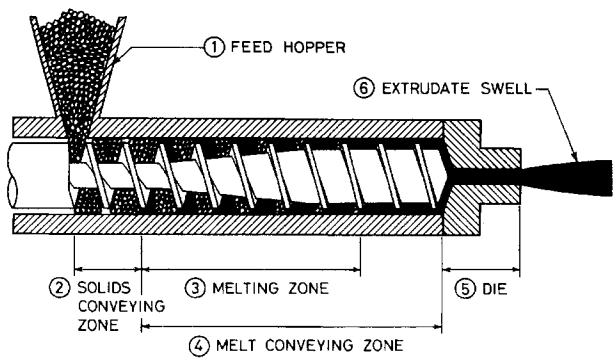

Fig. 1. Schematic diagram of a plasticating extruder showing the components of the present computer model.

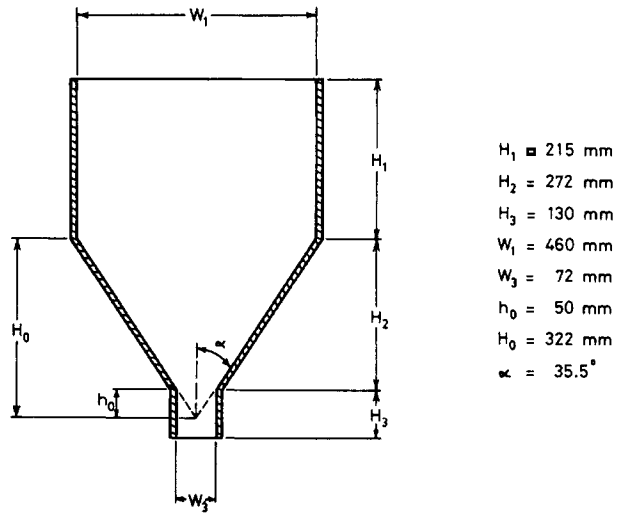

Fig. 2. Geometry and dimensions of a feed hopper with square cross-section.

relating the average vertical stress with the vertical stress near the wall (and assumed to be unity as a first approximation), δ the effective angle of friction of the solid particles, and f'_w the static coefficient of friction at the hopper wall.

Convergent Section:

$$p = \left(\frac{h_o}{H_o}\right)^{\psi} p_o + \frac{\rho_{bulk}g\,h_o}{\psi - 1} + \left[1 - \left(\frac{h_o}{H_o}\right)^{\psi-1}\right] \quad (2)$$

where

$$\psi = \frac{2B'D^*}{\tan\alpha}$$

$$B' = \frac{\sin\delta \sin(2\alpha + \kappa_o)}{1 - \sin\delta\cos(2\alpha + \kappa_o)}$$

$$\kappa_o = \beta_w + \arcsin\left(\frac{\sin\beta_w}{\sin\delta}\right), \arcsin < \frac{\pi}{2}$$

$$\beta_w = \arctan(f'_w)$$

and where p and p_o are the pressures at the base and top of the convergent section, h_o and H_o are the heights in the convergent section (as shown in *Fig. 2*), and 2α is the hopper angle.

Solids Conveying Zone

The solids-conveying mechanism in screw extruders is one of drag-induced flow; that is, flow due to the frictional drag of the barrel and screw surfaces on the solid polymer granules. Darnell and Mol (9) were the first to obtain solutions for the solids-conveying zone in screw extruders. More recently, there have been various refinements applied to their one-dimensional plug flow model by Schneider (10), Tadmor and Broyer (11, 12), and Lovegrove and Williams (13-15).

In the solids-conveying model described here, we assume that the solid bed is isothermal and travels as a solid plug with constant velocity. The stress distribution is assumed to be isotropic; that is, the pressure varies only in the downstream direction. By applying a force and torque balance on a differential element of the solid bed in the down-channel direction, the pres-

sure in the solids conveying zone is expressed in the form:

$$p = p_o\, e^{-\lambda z_b} \tag{3}$$

where

$$\lambda = \frac{A_1 K - B_1}{A_2 K + B_2}$$

$$A_1 = f_b W_b \sin\phi + 2Hf_s \sin\theta_b + W_s f_s \sin\theta_b$$

$$A_2 = HW_a \sin\theta_a$$

$$B_1 = f_b W_b \cos\phi - 2Hf_s \frac{D_a}{D_b} \sin\theta_b \operatorname{cotan}\theta_a - W_s f_s \frac{D_s}{D_b} \sin\theta_b \operatorname{cotan}\theta_s$$

$$B_2 = HW_a \frac{D_a}{D_b} \cos\theta_a$$

$$K = \frac{D_a}{D_b} \frac{\sin\theta_a + f_s \cos\theta_a}{\cos\theta_a - f_s \sin\theta_a}$$

and where p_0 is the base pressure in the feed hopper, z_b is down-channel distance at the barrel surface in the solids-conveying zone (as shown in *Fig. 3*), f_b and f_s are the dynamic coefficients of friction between the solid polymer particles and the barrel and screw surfaces, H is the screw channel depth, W_b and W_s are the channel widths at the barrel surface and screw root, θ_b and θ_s are the helix angles at the barrel surface and screw root, D_b is the inside diameter of the barrel, D_s is the outside diameter of the screw at the root, and W_a, D_a, and θ_a are (respectively) the average channel width, diameter, and helix angle measured at the midpoint between the barrel and screw-root surfaces. The angle ϕ, formed between the tangential velocity of the barrel surface and the down-channel velocity of the solid particles, is given by:

$$\tan\phi = \frac{\tan\theta_b}{\frac{\pi^2 N}{G} \rho_{bulk} HD_b(D_b - H) \tan\theta_b \left(\frac{W_a}{W_a + e}\right) - 1} \tag{4}$$

where N is the frequency of screw rotation, G is the mass flow rate of the polymer solids, and e is the screw fight width.

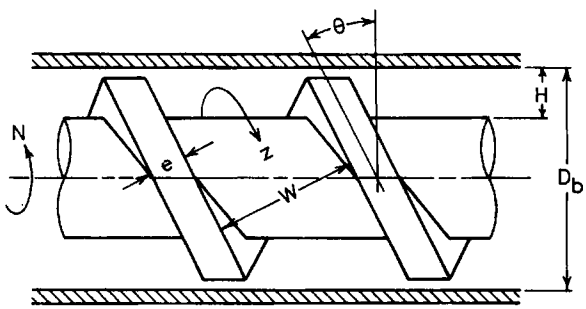

Fig. 3. Geometry of an extruder screw showing characteristic dimensions.

Melting Zone

The melting mechanism in screw extruders was first formulated by Tadmor (4, 5, 16) on the basis of visual observations. More sophisticated models have since been reported by Edmondson and Fenner (17), Shapiro, *et al.* (18, 19), the Lindt (20, 21). In the melting zone, the solid and melt phases coexist. The two phases are clearly segregated from each other, with the melt phase accumulating in a melt pool at the rear flight and the solids segregated as a solid bed at the front flight as, illustrated in *Fig. 4*. In addition, there exists a thin film of melt between the barrel surface and the solid bed. Due to the proximity of the heated barrel and the intense shear, much of the melting occurs in this melt film. The motion of the barrel relative to the solid bed drags the melt in this film into the melt pool. The width of the melt pool gradually increases in the down-channel direction.

Tadmor's melting model has been used as a basis for the model described in this paper. The delay in melting (that is, the down-channel distance between the start of barrel heating and the appearance of the melt pool) is obtained from an empirical correlation based on experimental data (4). It is assumed that the downstream bed velocity is constant and that the thickness of the upper melt film is independent of cross-channel position. A temperature- and shear-rate-dependent viscosity relation is used to calculate the temperature profile in the melt film. Mass and energy balances on the melt film and solid bed are carried out to obtain the following equations for the rate of melting and the solid-bed profile (22):

Rate of melting:

$$\omega = \Phi\left(\frac{dT}{dy}\right)_{y=0} X \tag{5a}$$

$$= \left|\frac{V_{bx}}{2}\right| \rho_m \delta \tag{5b}$$

where

$$\Phi = \frac{k_m}{Cp_s(T_{melt} - T_{sol}) + \lambda + Cp_m(T_{bulk} - T_{melt})}$$

$\left(\frac{dT}{dy}\right)_{y=0}$ = temperature gradient in the melt film at the solid-melt interface (and a function of the melt film thickness δ)

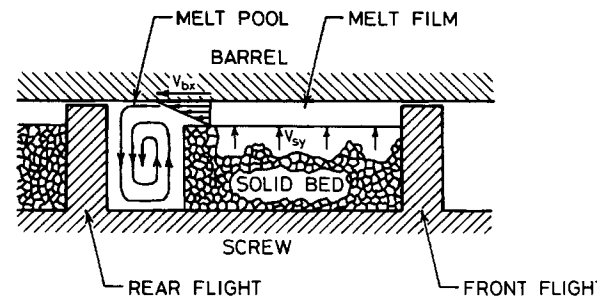

Fig. 4. Idealized cross-section of screw channel in the melting zone. V_{bx} is the component of barrel velocity in the cross channel direction, and V_{sy} is the velocity of the solid bed moving into the solid-melt interface.

and where X is the width of the solid bed, V_{bx} is the cross-channel component of the barrel velocity, T_{bulk} is the flow-average (bulk) temperature of the melt film, T_{melt} is the melting temperature of the polymer, T_{sol} is the temperature of the solid bed far away from the interface, ρ_m is the melt density, Cp_m and Cp_s are the specific heats of the polymer melt and solid, respectively, k_m is the thermal conductivity of the melt, and λ is the heat of fusion of the polymer.
Solid bed profile:

$$\frac{d(H^*X)}{dz} = \frac{-\omega}{\rho_s V_{sz}} = \frac{-\Phi}{\rho_s V_{sz}} \left(\frac{dT}{dy}\right)_{y=0} X \quad (6)$$

where $H^* = H - \delta$, ρ_s is the solid polymer density, and V_{sz} is the down-channel velocity of the solid bed. *Equations 5b* and *6* are solved simultaneously using a fourth-order Runge-Kutta method to obtain the solid-bed profile X/W as a function of the down-channel direction in the screw channel.

Melt Conveying Zone

Two distinct melt-conveying regions may be found in plasticating extruders. One is downstream of the melting zone after completion of melting and occupies the entire width of the screw channel. The other occurs in the melt pool, extending side by side with the solid bed in the melting zone. Here, the width of the melt pool changes in the down-channel direction. The mass flow rate of the melt also changes as a result of the influx from the melt film.

Due to the helical geometry of the extruder screw and the relative motions of the barrel and screw, the flow pattern of the polymer melt in the screw channel is quite complex and may be described as a "helix within a helix." In order to solve this complex flow problem, several simplifying assumptions are made. It is convenient to pick a coordinate system relative to the screw. Also, one may treat the barrel as rotating about a stationary screw, a valid procedure because gravity and centrifugal inertia forces are negligible in comparison with viscous and pressure forces in the screw channel. Another standard assumption is to consider the helical screw channel as "unwound" and rectilinear. This is a valid assumption because, in most single-screw extruders, the screw channel is relatively shallow in the melt-flow regions. In the analysis of melt flow, it is also standard procedure to introduce the lubrication approximation (23). This involves the local replacement of the actual flow in the parallel or nearly parallel gap between smooth surfaces by uniform flow between plane parallel surfaces.

As stated earlier in this article, by far the majority of studies on extrusion theory in the literature have dealt with the analysis of melt flow. Griffith (24), Zamodits and Pearson (25), and Fenner (6) obtained numerical solutions for fully developed, two-dimensional, nonisothermal, and non-Newtonian flow of melts in infinitely wide rectangular screw channels. For a similar type of flow, Martin (26) presented a solution that allows for the finite width of the channel. Yates (27) and Fenner (28) have developed two-dimensional, nonisothermal, and non-Newtonian solutions for infinitely wide rectangular screw channels in which the temperature profiles are developing along the channel. For a more complete discussion of extruder models, one is referred to a review by Fenner (7) that, in addition to melt flow in extruders, also covers the analysis of solids conveying and melting.

In the melt-conveying model described here, the following equations of conservation of mass, momentum, and energy in simplified form, together with the accompanying boundary conditions, are solved simultaneously.

Mass (integrated form):

$$\int_0^H v_x \, dy = 0 \quad (7)$$

$$\int_0^H v_z \, dy = \frac{Q}{W} \quad (8)$$

Momentum:

$$-\frac{\partial p}{\partial x} + \frac{\partial \tau_{yx}}{\partial y} = 0 \quad (9)$$

$$-\frac{\partial p}{\partial z} + \frac{\partial \tau_{yz}}{\partial y} = 0 \quad (10)$$

Energy:

$$\rho_m Cp_m v_z \frac{\partial T}{\partial z} = k_m \frac{\partial^2 T}{\partial y^2} + \tau_{yx} \frac{\partial v_x}{\partial y} + \tau_{yz} \frac{\partial v_z}{\partial y} \quad (11)$$

Boundary conditions:

$$\begin{array}{llll} z = 0 & p = p_o & & T = T_o \\ y = 0 & v_x = v_z = 0 & & T = T_b \\ y = H & v_x = V_{bx} & v_z = V_{bz} & T = T_b \end{array} \quad (12)$$

where Q/W is the flow rate of the melt per unit width of the flow channel, p_o and T_o are the pressure and temperature, respectively, at the beginning of the melt flow region, T_b is the barrel temperature (which may also be specified as a function of the down-channel direction), and V_{bx} and V_{bz} are the cross- and down-channel components of the barrel velocity. The following temperature- and shear-rate-dependent constitutive relation is used:

$$\tau_{yx} = \eta \frac{\partial v_x}{\partial y} \quad (13)$$

$$\tau_{yz} = \eta \frac{\partial v_z}{\partial y} \quad (14)$$

$$\log \eta = a_o + a_1 \log \dot{\gamma} + a_2 (\log \dot{\gamma})^2 + a_3 T + a_4 T^2 + a_5 T \log \dot{\gamma} \quad (15)$$

where

$$\dot{\gamma} = \sqrt{\left(\frac{\partial v_x}{\partial y}\right)^2 + \left(\frac{\partial v_z}{\partial y}\right)^2}$$

The viscosity relation is obtained by curve-fitting Instron capillary rheometer data, as shown in *Figs. 5* and *6*, to *Eq 15* using linear regression. It should be noted that, by retaining the convective term in the en-

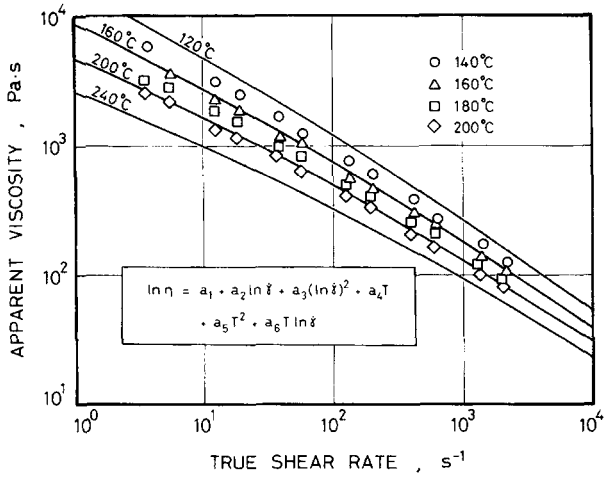

Fig. 5. Viscosity curves for LDPE. Data points represent viscosities measured with an Instron capillary rheometer. Solid curves denote the general viscosity equation (see inset)–parameters a_1 to a_6 are obtained by linear regression.

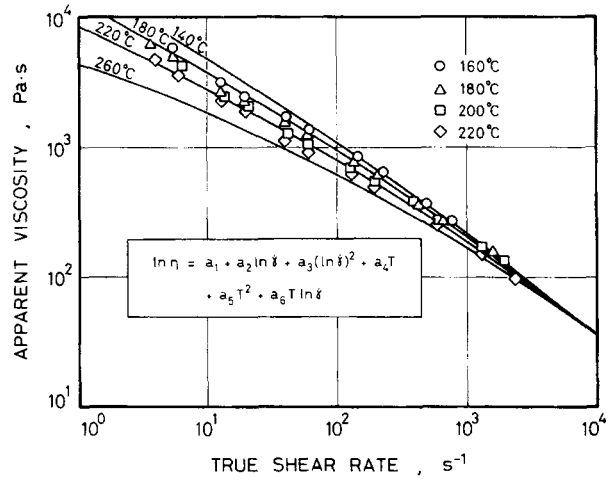

Fig. 6. Viscosity curves for HDPE. Data points represent viscosities measured with an Instron capillary rheometer. Solid curves denote the general viscosity equation (see inset)–parameters a_1 to a_6 are obtained by linear regression.

ergy equation, developing temperature profiles along the screw channel are calculated.

The conservation equations shown above are solved by an implicit finite-difference technique to obtain cross- and down-channel velocity profiles, temperature profiles, and the down-channel pressure profile (22). In addition to viscosity, the polymer properties required for the model are thermal conductivity, density, and specific heat of the melt.

Breaker Plate, Adapter, and Die

The adapter and die used in this study are illustrated in *Figs.* 7 and 8. The adapter contains a 3/4 in. x 3/8 in. (19.1 mm x 9.5 mm) rectangular slit channel, whereas the die has a 3/16 in. (4.76 mm) diameter channel of circular cross-section. For the breaker plate, adapter, and die, the melt-flow analysis is essentially the same as described for the melt-conveying section of the extruder, with the exception that only the down-channel components of velocity are considered and that there are no moving boundaries. The following conservation

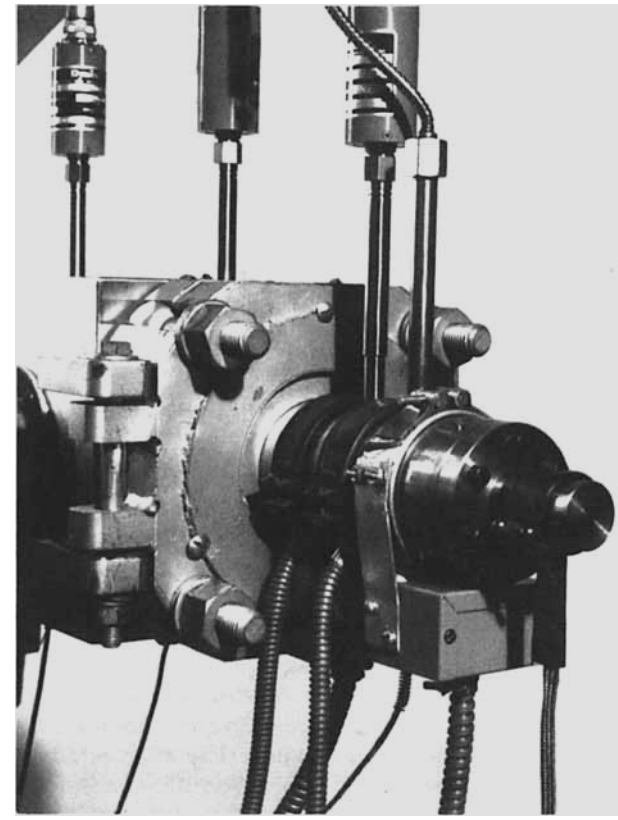

Fig. 7. Photograph of adapter and die.

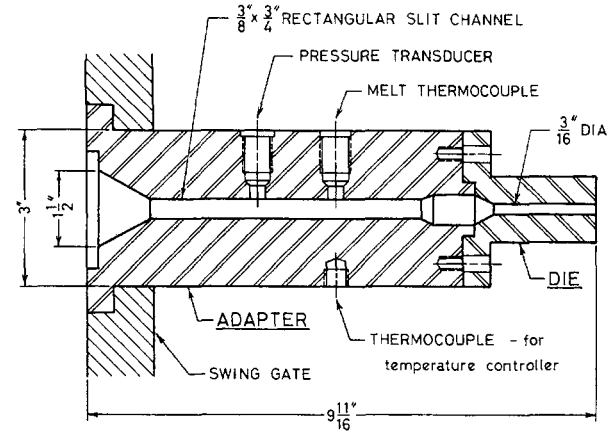

Fig. 8. Schematic diagram of adapter and die.

equations, in simplified form, for the breaker plate, adapter, and die are solved simultaneously:

Breaker Plate

Mass (integrated form):

$$\int_0^{R_{Br}} v_z\, r\, dr = \frac{Q}{2\pi N_{Br}} \tag{16}$$

Momentum:

$$-\frac{\partial p}{\partial z} + \frac{1}{r}\frac{\partial}{\partial r}(r\tau_{rz}) = 0 \tag{17}$$

Energy:

$$\rho_m Cp_m v_z \frac{\partial T}{\partial z} = \frac{k_m}{r}\frac{\partial}{\partial r}\left(r\frac{\partial T}{\partial r}\right) + \tau_{rz}\frac{\partial v_z}{\partial r} \tag{18}$$

Boundary conditions:

$$\begin{aligned} z = 0 \quad & p = p_o \quad & T = T_o \\ r = 0 \quad & \frac{\partial v_z}{\partial r} = 0 \quad & \frac{\partial T}{\partial r} = 0 \\ r = R_{Br} \quad & v_z = 0 \quad & \frac{\partial T}{\partial r} = 0 \end{aligned} \tag{19}$$

where N_{Br} is the number of holes in the breaker plate, R_{Br} is the radius of each hole, and p_o and T_o are the pressure and bulk temperature of the polymer melt at the end of the extruder screw channel.

Adapter

Mass (integrated form):

$$\int_o^{H_A/2} v_z \, dy = \frac{Q}{2W_A} \tag{20}$$

Momentum:

$$-\frac{\partial p}{\partial z} + \frac{\partial \tau_{yz}}{\partial y} = 0 \tag{21}$$

Energy:

$$\rho_m \, Cp_m \, v_z \frac{\partial T}{\partial z} = k_m \frac{\partial^2 T}{\partial y^2} + \tau_{yz} \frac{\partial v_z}{\partial y} \tag{22}$$

Boundary conditions:

$$\begin{aligned} z = 0 \quad & p = p_o \quad & T = T_o \\ y = 0 \quad & \frac{\partial v_z}{\partial y} = 0 \quad & \frac{\partial T}{\partial y} = 0 \\ y = \frac{H_A}{2} \quad & v_z = 0 \quad & T = T_A \end{aligned} \tag{23}$$

where H_A and W_A are (respectively) the height and width of the rectangular flow channel, p_o and T_o are the pressure and bulk temperature of the melt at the end of the breaker plate, and T_A is the temperature of the adapter.

Die

Mass (integrated form):

$$\int_o^{RD} v_z \, r \, dr = \frac{Q}{2\pi} \tag{24}$$

Momentum:

$$-\frac{\partial p}{\partial z} + \frac{1}{r}\frac{\partial}{\partial r}(r\tau_{rz}) = 0 \tag{25}$$

Energy:

$$\rho_m \, Cp_m \, v_z \frac{\partial T}{\partial z} = \frac{k_m}{r}\frac{\partial}{\partial r}\left(r \frac{\partial T}{\partial r}\right) + \tau_{rz}\frac{\partial v_z}{\partial r} \tag{26}$$

Boundary conditions:

$$\begin{aligned} r = 0 \quad & \frac{\partial v_z}{\partial r} = 0 \quad & \frac{\partial T}{\partial r} = 0 \\ r = R_D \quad & v_z = 0 \quad & T = T_D \end{aligned} \tag{27}$$

where R_D is the radius of the circular flow channel in the die, and T_D is the die temperature.

An implicit finite-difference method is used to solve the conservation equations shown above to obtain velocity, temperature, and pressure profiles in the breaker plate, adapter, and die (22). As in the extruder screw channel, the polymer properties required for the calculations are viscosity, thermal conductivity, density, and specific heat of the melt.

Extrudate Swell

Polymer melts, due to their viscoelastic behavior, exhibit an increase in cross-sectional area whenever they emerge from a die, provided that there is no subsequent drawing. This phenomenon is usually called extrudate swell. Depending on the extrusion conditions, the die geometry and dimensions, and the rheological properties of the polymer, the increase in extrudate diameter (in the case of a circular die) may range from 1.5 to 4 times the die diameter.

There seems to be a general agreement that extrudate swell is mainly due to a sudden recovery of stored elastic energy and a subsequent stress relaxation. However, no single theory of extrudate swell seems to be generally accepted. A review paper by Vlachopoulos (29) has recently been published on extrudate swell of polymers. It is concluded that, despite the large number of investigations on extrudate swell, the existing models do not provide a clear picture as to the importance of the various rheological parameters. There is still disagreement regarding the molecular structure effects for many polymers. The interrelations between molecular, rheological, and geometrical parameters and their effect on extrudate swell are not well-understood. A fully predictive theory has yet to be developed.

In the model described here, the prediction of extrudate swell for the circular die is based on Tanner's elastic recovery theory (30), studies by White, *et al.* (31-33), and by Racin and Bogue (34), and measurements of extrudate swell performed on an Instron capillary rheometer. Tanner's equation for extrudate swell may be expressed as:

$$\frac{d}{D} = \left[\frac{\int_o^R \left(N_1 + G - \frac{\tau^2}{G}\right) r \, dr}{\int_o^R G \, r \, dr}\right]^{1/6} + 0.12 \tag{28}$$

where N_1 is the first normal stress difference, G is an elastic modulus, and τ is the shear stress. *Equation 28* may be written as:

$$\frac{d}{D} = \left[\frac{\int_o^{\tau w} \left[N_1(\tau) + G(\tau) - \frac{\tau^2}{G(\tau)}\right] \tau d\tau}{\int_o^{\tau w} G(\tau) \, \tau \, d\tau}\right]^{1/6} + 0.12 \tag{29}$$

Assuming that:

$$N_1 = A\tau^b \tag{30}$$

$$G = \frac{2\tau^2}{N_1} \tag{31}$$

and substituting *Eqs 30* and *31* into *Eq 29*, one obtains the following equation for the prediction of extrudate swell for an extruder die with circular cross-section:

$$\frac{d}{D} = \left[\frac{A^2}{4}\frac{(4-b)}{(2+b)}\tau_w^{2b-2} + 1\right]^{1/6} + 0.12 \quad (32)$$

The parameters A and b are obtained by curve-fitting *Eq 32* to the Instron capillary extrudate swell data using nonlinear regression, as shown in *Figs. 9* and *10*.

RESULTS OF SIMULATIONS AND EXPERIMENTS

The present computer model was used to simulate a 1½ in. (38 mm) diameter, 24:1 L/D single-screw plasticating extruder. Various screw speeds and barrel-temperature profiles were used for both high- and low-density polyethylene resin. The simulations were confirmed with experimental runs on a Killion single-screw extruder. For each run, pressure measurements at three locations (two in the screw channel and one in the adapter) were obtained using Dynisco transducers, and the melt temperature was measured in the adapter using a melt thermocouple. The mass-flow rate of the polymer and the extrudate swell at the die exit were also measured.

Results of the computer simulations and experimental measurements are presented in *Tables 1* to *4* and

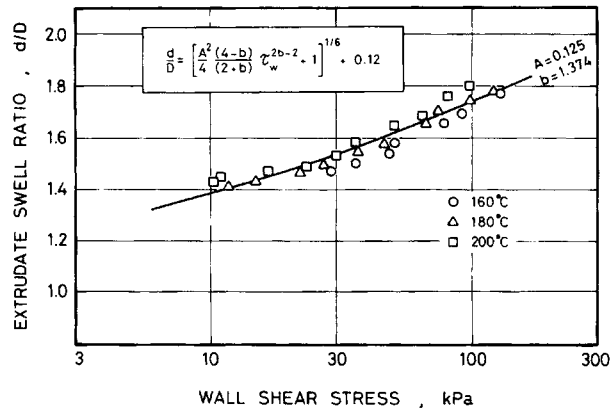

Fig. 9. Extrudate swell correlation for LDPE. Data points represent extrudate swells measured on an Instron capillary rheometer. Solid curve denotes the extrudate swell equation (see inset)–parameters A and b are obtained by nonlinear regression.

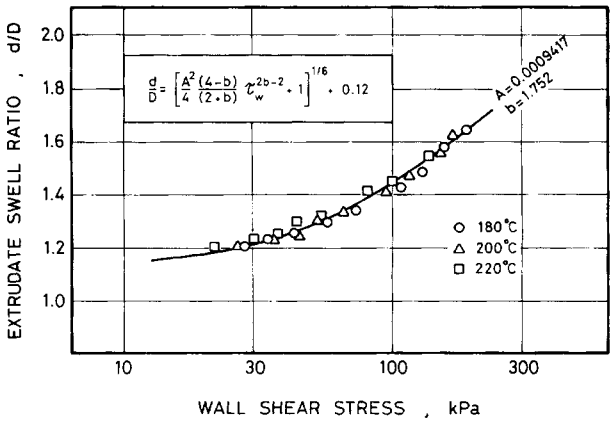

Fig. 10. Extrudate swell correlation for HDPE. Data points represent extrudate swells measured on an Instron capillary rheometer. Solid curve denotes the extrudate swell equation (see inset)–parameters A and b are obtained by nonlinear regression.

Table 1. Predicted vs. Measured Mass-Flow Rates for LDPE

Screw speed, rpm	Mass-flow rate, kg/s	
	Predicted	Measured
40	$1.965 \cdot 10^{-3}$	$1.911 \cdot 10^{-3}$
60	$2.929 \cdot 10^{-3}$	$2.948 \cdot 10^{-3}$
80	$3.886 \cdot 10^{-3}$	$3.968 \cdot 10^{-3}$

Table 2. Predicted vs. Measured Mass-Flow Rates for HDPE

Screw speed, rpm	Mass-flow rate, kg/s	
	Predicted	Measured
40	$1.881 \cdot 10^{-3}$	$1.755 \cdot 10^{-3}$
60	$2.812 \cdot 10^{-3}$	$2.707 \cdot 10^{-3}$
80	$3.748 \cdot 10^{-3}$	$3.705 \cdot 10^{-3}$

Table 3. Predicted vs. Measured Extrudate Swell for LDPE

Screw speed, rpm	Extrudate swell, d/D	
	Predicted	Measured
40	1.692	1.646
60	1.721	1.674
80	1.742	1.713

Table 4. Predicted vs. Measured Extrudate Swell for HDPE

Screw speed, rpm	Extrudate swell, d/D	
	Predicted	Measured
40	1.692	1.646
60	1.721	1.674
80	1.742	1.713

Figs. 11 to *16* for two polymers: low-density polyethylene (Union Carbide Canada Ltd., DFDY 4400) and high-density polyethylene (DuPont Canada Inc., SCLAIR 19A). The extruder screw dimensions, processing conditions, and polymer properties are listed in *Tables 5* to *7*. The feed hopper and die dimensions are given in *Figs. 2* and *8*, respectively.

In *Tables 1* and *2*, the predicted and measured mass-flow rates for LDPE and HDPE are compared at three

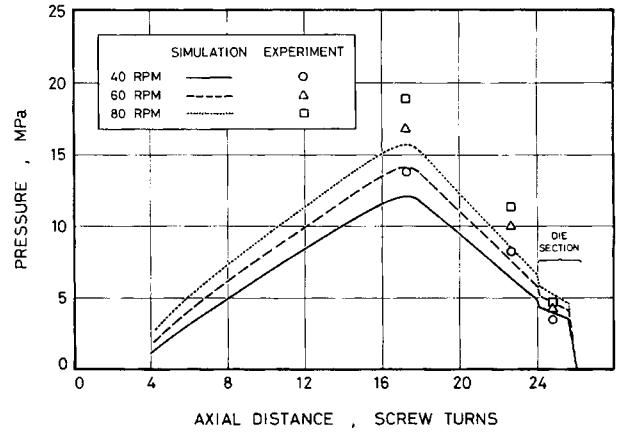

Fig. 11. Predicted down-channel pressure profiles in the extruder screw channel and die section for LDPE. Data points represent melt-pressure measurements in the extruder and adapter.

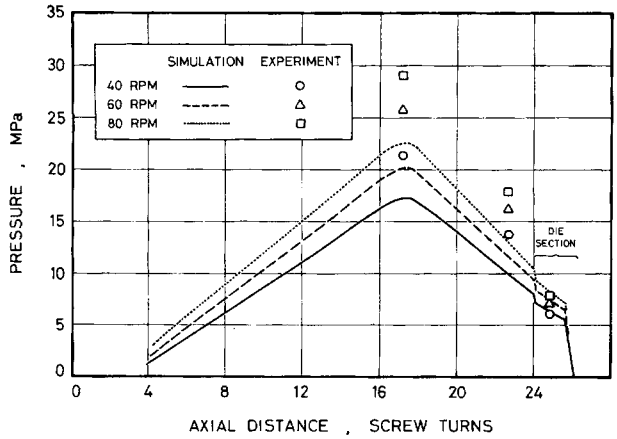

Fig. 12. Predicted down-channel pressure profiles in the extruder screw channel and die section for HDPE. Data points represent melt-pressure measurements in the extruder and adapter.

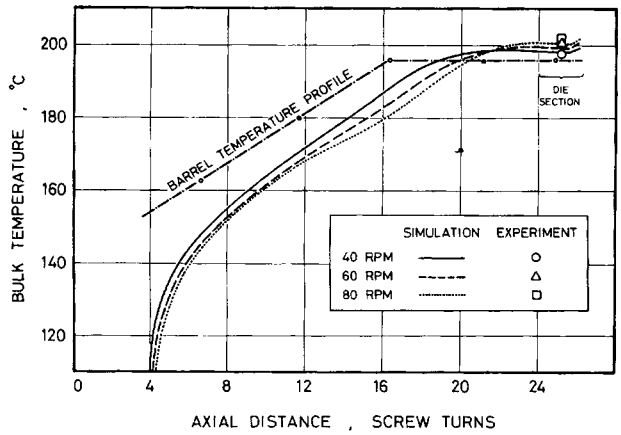

Fig. 13. Predicted down-channel bulk temperature profiles in the extruder screen channel and die section of LDPE. Data points represent melt temperature measurements in the adapter.

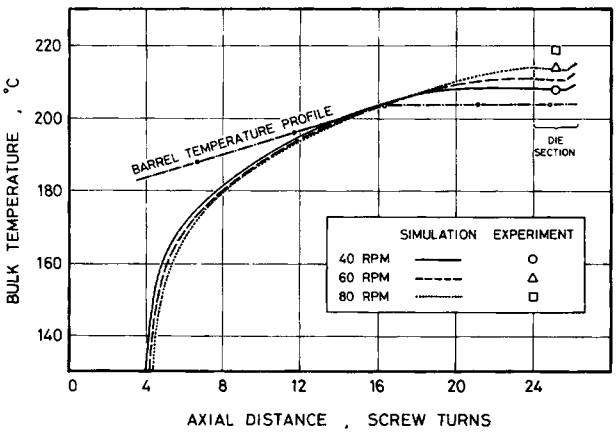

Fig. 14. Predicted down-channel bulk temperature profiles in the extruder screw channel and die section for HDPE. Data points represent melt temperature measurements in the adapter.

frequencies of screw rotation: 40, 60, and 80 rpm. In the case of the LDPE, the predicted and measured values differ by 1 to 3 percent; for the HDPE, the difference ranges between 1 and 7 percent. Down-channel pressure profiles for the two resins are presented in *Figs. 11* and *12*, and are compared with the melt pressure measurements in the extruder and adapter. As compared to the measured pressure values, the predicted profiles are lower in the screw channel and higher in the adapter. The differences range between 12 and 25 percent for the LDPE, and between 7 and 27 percent for the HDPE. In *Figs. 13* and *14*, the down channel bulk temperature profiles for the two resins are presented, along with the melt temperature measurements in the adapter. The difference between the predicted and measured temperature values range between 1° and 2°C for the LDPE, and between 1° and 5°C for the HDPE. No measurements of melt temperature were made in the extruder screw channel. Predicted solid-bed profiles are shown in *Figs. 15* and *16* for the two resins. However, experimental verification of these predictions was not performed. Finally, the predicted and measured values of extrudate swell at the die exit are compared in *Tables 3* and *4*. The difference between the predicted and measured values is approxi-

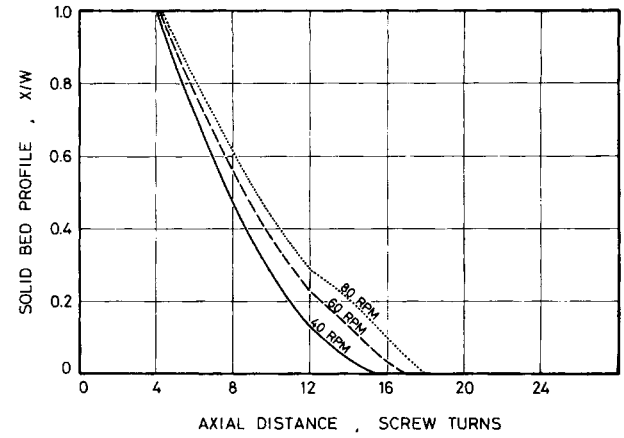

Fig. 15. Predicted solid-bed profiles in the extruder screw channel for LDPE.

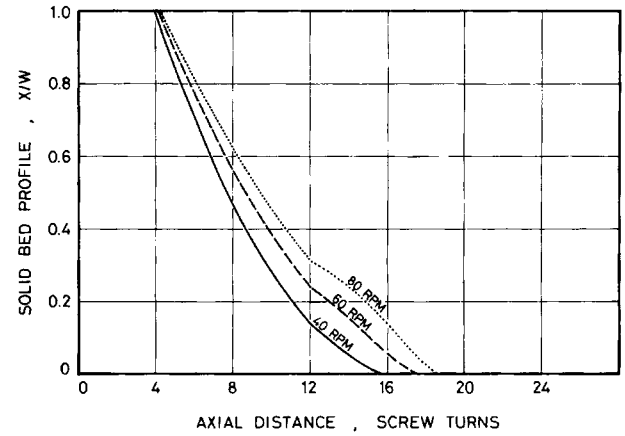

Fig. 16. Predicted solid-bed profiles in the extruder screw channel for HDPE.

Table 5. Extruder Screw Geometry and Dimensions

Square-pitch screw	
Feed/compression/metering sections	12/6/6 turns
Barrel inside diameter, D_b	1.50 in. (38.1 mm)
Screw lead	1.50 in. (38.1 mm)
Channel depth in feed section	0.24 in. (6.1 mm)
Channel depth in metering section	0.08 in. (2.0 mm)
Flight width	0.25 in. (6.35 mm)

Table 6. Material Properties and Processing Variables for LDPE (Union Carbide Canada Ltd., DFDY 4400)

Extruder operating conditions		
Barrel temperature profile		163/179/196/196/196°C
Frequency of screw rotation		40, 60, and 80 rpm
Material and rheological properties		
Static coefficient of friction, f'_w		0.30
Effective angle of friction, δ		33.7°
Dynamic coefficient of friction, f_b		0.40
Dynamic coefficient of friction, f_s		0.25
Heat capacity—melt, Cp_m		2595 J/(kg · K)
—solid, Cp_s		2763 J/(kg · K)
Density—bulk, ρ_{bulk}		595 kg/m³
—melt, ρ_m		779 kg/m³
—solid, ρ_s		919 kg/m³
Thermal conductivity—melt, k_m		0.182 W/(m · K)
Heat of fusion, λ		129785 J/kg
Melting temperature, T_{melt}		110°C
Viscosity, η (see Fig. 5)	a_1	11.7838
	a_2	−0.639104
	a_3	−0.0112744
	a_4	−0.0183449
	a_5	$8.78448 \cdot 10^{-6}$
	a_6	$9.66512 \cdot 10^{-4}$
where η[Pa · s], $\dot{\gamma}$[s⁻¹], T[°C]		
Extrudate swell correlation (see Fig. 9)	A	0.125
	b	1.374

Table 7. Material Properties and Processing Variables for HDPE (DuPont Canada Inc., SCLAIR 19A)

Extruder operating conditions		
Barrel temperature profile		188/196/204/204/204°C
Frequency of screw rotation		40, 60, and 80 rpm
Material and rheological properties		
Static coefficient of friction, f'_w		0.30
Effective angle of friction, δ		33.7°
Dynamic coefficient of friction, f_b		0.40
Dynamic coefficient of friction, f_s		0.25
Heat capacity—melt, Cp_m		2512 J/(kg · K)
—solid, Cp_s		2303 J/(kg · K)
Density—bulk, ρ_{bulk}		595 kg/m³
—melt, ρ_m		777 kg/m³
—solid, ρ_s		960 kg/m³
Thermal conductivity—melt, k_m		0.182 W/(m · K)
Heat of fusion, λ		201189 J/kg
Melting temperature, T_{melt}		130°C
Viscosity, η (see Fig. 6)	a_1	9.95345
	a_2	−0.782449
	a_3	−0.0114677
	a_4	$4.50087 \cdot 10^{-3}$
	a_5	$-3.93029 \cdot 10^{-5}$
	a_6	$1.41590 \cdot 10^{-3}$
where η[Pa · s], $\dot{\gamma}$[s⁻¹], T[°C]		
Extrudate swell correlation (see Fig. 10)	A	$9.417 \cdot 10^{-4}$
	b	1.752

mately 2 percent for the LDPE and 10 percent for the HDPE.

Further refinements of the extruder model, especially in the solids-conveying zone and in the initial stages of the melt-conveying zone, should minimize the differences between the predicted and measured values given above. A parameter sensitivity study was also performed for each of the polymer properties utilized in the overall model. The polymer property data were individually changed by 2 percent, and their effect on the overall extruder performance was examined in each case. It was seen that changes in the dynamic coefficients of friction and melt density had the greatest effect, especially on mass-flow rate and pressure development in the extruder screw channel. More accurate values of these properties would also improve the overall extruder model results.

CONCLUDING REMARKS

A fully-predictive computer model for a single-screw plasticating extruder has been developed to predict the flow rate of the polymer, pressure, and temperature profiles along the extruder flow channel in the die and in the extrudate swell at the die exit. The simulations depend entirely on the material and rheological properties of the polymer, the screw geometry and dimensions, and the operating conditions of the extruder (screw speed and barrel-temperature profile). The simulations are not modified on the basis of temperature or pressure measurements in the extruder. Any size of extruder or screw design within reasonable limits may be simulated by the present computer model.

Finally, it is possible to further improve the overall computer model by improving the individual submodels, especially for the solids-conveying, delay in melting, and the melting sections. However, to improve these submodels, we need more direct experimental evidence on exactly what happens in these subsections. Presently, we cannot justify introducing more sophisticated models until such information becomes available. Also, the additional computation time that may be necessary for the model will be a factor to be considered when introducing such improvements.

ACKNOWLEDGMENTS

The authors gratefully acknowledge the Natural Sciences and Engineering Research Council of Canada for financial assistance, and DuPont Canada Inc. and Union Carbide of Canada, Limited for their donations of the polyethylene resins used in the experimental runs.

NOMENCLATURE

Cp	= specific heat
d/D	= extrudate swell ratio
D_b, D_s	= screw diameter at barrel surface and at screw root
e	= screw flight width (perpendicular to the flight)
f_b, f_s	= dynamic coefficient of friction at barrel and screw surface
f'_w	= static coefficient of friction at feed-hopper wall
g	= gravitational acceleration
G	= mass-flow rate
G	= elastic modulus
H	= screw-channel depth
k	= thermal conductivity
N	= frequency of screw rotation
N_1	= first normal stress difference
p	= pressure
Q	= volumetric flow rate
r	= radial distance in cylindrical coordinates
R	= radius
T	= temperature
T_{bulk}	= bulk (flow-average) temperature

T_{melt} = melting temperature of polymer
v_x, v_z = cross-channel and down-channel velocity
V_b = tangential barrel velocity
W = screw-channel width (perpendicular to flight)
x = cross-channel distance
X = solid-bed width
X/W = solid-bed profile
y = distance perpendicular to x- and z-directions
z = down-channel distance
$\dot{\gamma}$ = shear rate
δ = effective angle of friction
δ = thickness of melt film in melting zone
η = non-Newtonian viscosity
θ = helix angle
λ = latent heat of fusion
ρ = density
τ, τ_{yx}, τ_{yz} = shear stress
ω = rate of melting per unit down-channel distance

REFERENCES

1. E. C. Bernhardt, ed., "Processing of Thermoplastic Materials," Reinhold, New York (1959).
2. J. M. McKelvey, "Polymer Processing," Wiley, New York (1962).
3. I. Klein and D. I. Marshall, eds., "Computer Programs for Plastics Engineers," Reinhold, New York (1968).
4. Z. Tadmor and I. Klein, "Engineering Principles of Plasticating Extrusion," Reinhold, New York (1970).
5. Z. Tadmor and C. G. Gogos, "Principles of Polymer Processing," Wiley-Interscience, New York (1979).
6. R. T. Fenner, "Extruder Screw Design," Iliffe, London (1970).
7. R. T. Fenner, *Polymer*, **18**, 617 (1977).
8. D. M. Walker, *Chem. Eng. Sci.*, **21**, 975 (1966).
9. W. H. Darnell and E. A. J. Mol, *SPE J.*, **12**, 20 (April 1956).
10. K. Schneider, "Technical Report on Plastics Processing —Processes in the Feeding Zone of an Extruder," Institute of Plastics Processing (IKV), Aachen (1969).
11. E. Broyer and Z. Tadmor, *Polym. Eng. Sci.*, **12**, 12 (1972).
12. Z. Tadmor and E. Broyer, *Polym. Eng. Sci.*, **12**, 378 (1972).
13. J. G. A. Lovegrove and J. G. Williams, *J. Mech. Eng. Sci.*, **15**, 114 (1973).
14. J. G. A. Lovegrove and J. G. Williams, *J. Mech. Eng. Sci.*, **15**, 195 (1973).
15. J. G. A. Lovegrove and J. G. Williams, *Polym. Eng. Sci.*, **14**, 589 (1974).
16. Z. Tadmor, *Polym. Eng. Sci.*, **6**, 185 (1966).
17. I. R. Edmondson and R. T. Fenner, *Polymer*, **16**, 49 (1975).
18. J. Shapiro, A. L. Halmos, and J. R. A. Pearson, *Polymer*, **17**, 905 (1976).
19. A. L. Halmos, J. R. A. Pearson, and R. Trottnow, *Polymer*, **19**, 1199, (1978).
20. J. T. Lindt, *Polym. Eng. Sci.*, **16**, 284 (1976).
21. J. T. Lindt, *Polym. Eng. Sci.*, **21**, 1162 (1981).
22. E. E. Agur, Ph.D. Thesis, McMaster University, Hamilton, Canada (1982).
23. J. R. A. Pearson, "Mechanical Principles of Polymer Melt Processing," Pergamon, Oxford (1966).
24. R. M. Griffith, *Ind. Eng. Chem. Fundam.*, **1**, 180 (1962).
25. H. J. Zamodits and J. R. A. Pearson, *Trans. Soc. Rheol.*, **13**, 357 (1969).
26. B. Martin, Ph.D. Thesis, Cambridge University (1969).
27. B. Yates, Ph.D. Thesis, Cambridge University (1968).
28. R. T. Fenner, *Polymer*, **16**, 298 (1975).
29. J. Vlachopoulos, *Rev. Def. Beh. Mat.*, **3**, 219 (1981).
30. R. I. Tanner, *J. Polym. Sci.*, **A2, 8**, 2067 (1970).
31. J. L. White, *Trans. Soc. Rheol.*, **19**, 271 (1975).
32. J. L. White and J. F. Roman, *J. Appl. Polym. Sci.*, **20**, 1005 (1976); *ibid.*, **21**, 869 (1977).
33. D. C. Huang and J. L. White, *Polym. Eng. Sci.*, **19**, 609 (1979).
34. R. Racin and D. C. Bogue, *J. Rheol.*, **23**, 263 (1979).

Discussion of the E. E. Agur Article

W. I. Patterson. This morning we heard Dr. Kamal talk of modeling of injection molding, one of the important achievements that exists for predicting short shots. In modeling extruders, one would want a model that would predict surging. I wonder if your model can do this. Could you comment upon how models could predict extruder surging?

E. E. Agur. Surging cannot be predicted by our model. This is related to the melting model that we have selected. The model assumes a constant velocity of the solid bed in the screw channel. In order to predict surging, one should allow for the acceleration of the solid bed.

Ch. I. Chung. I have two questions. Firstly, in solid conveying, you said that you used the Darnell and Mol equation, in which you need to insert an initial pressure. Depending on the choice of the initial pressure, one can get all sorts of outputs. How did you select this initial pressure? Secondly, in the melting zone, the Tadmor model that you have used assumes a constant solid-plug velocity. For this reason, in order to make pressure computation, you have to make some assumptions again. Here also, depending on what you do, your results will vary. How did you calculate the pressure profile that eventually gave you such a good fit in the output data?

E. E. Agur. First of all, we predicted the pressure at the start of the solids conveying zone by calculating the base pressure at the bottom of the feed-hopper. The whole purpose of adding the feed-hopper to the model was to allow us to calculate the base pressure. As for the pressure profile in the solid-conveying zone, one has to assume a mass-flow rate of the polymer. This assumed value was maintained through the length of the extruder. Using it, we calculated the pressure profile in the solids bed, the pressure profile in the melting and metering zones, and then, finally, the final pressure at the unit of the die. If the computed exit pressure was greater than zero, then we had to assume a new mass flow rate and repeat the calculation until zero exit pressure was obtained.

Ch. I. Chung. In the melting section, you are calculating the pressure profile. However, here you cannot apply the friction model because the polymer is melting. How did you calculate the pressure in this case?

E. E. Agur. We started the melt-conveying zone in parallel with the melting zone. We calculated a pressure profile in the melt pool, and then this was carried in parallel with the melting zone.

V. L. Lenir. Could you give some details are to how you started off this melting zone? I assumed some sort of a delay time. The melt pulled over the top of the solid plug had to reach a certain proportion of the flight clearance.

E. E. Agur. We employed the same method and correlation, as proposed by Tadmor.

V. L. Lenir. You did not take into account the height of the channel. There are two factors that were used by Tadmor, called F_d and F_p, to account for the shape of the flight. Your model assumes an infinite channel width. Is there not any scope for doing some sort of curve fitting for these two factors against the ratio of the channel height to the channel width for non-Newtonian systems?

E. E. Agur. As long as one deals with Newtonian fluids, then it is possible to combine the shape factors for drag and pressure flow in some manner. However, for non-Newtonian systems, it is not possible to obtain simple analytical expressions for the shape factors. Some workers have obtained some numerical correlations between shape factors and aspect ratio for such a situation. In our case, we did not pursue this matter. We discovered that using Newtonian shape factors to deal with a non-Newtonian extrusion situation caused more problems than it solved.

V. L. Lenir. You assumed plug flow in the solids feed zone. One would not except this to be valid with powder feed. This means that your model applies mainly for pellets.

E. E. Agur. Yes.

L. A. Utracki. From the point of view of rheology, the assumption that only the shear viscosity is to be taken into account is wrong. As I understand it, you are disregarding even the variation of viscosity with pressure. For some polymers, an increase of pressure by 1 kbar changes viscosity by a factor of 1,000. Furthermore, there are experimental data that show that, for two resins having nearly identical shear flow curves, the extruder output varies with normal stress. Nevertheless, the agreement between theory and the data that you presented is astonishing. The question is: why? Obviously, you have two adjustable parameters for the die swell, but for the extruder output, you do not seem to have any adjustable parameters.

M. R. Kamal. I want to insert one more question. What kind of P-V-T relation did you use, and what kind of variation of properties, besides viscosity, did you allow in your model? Did you consider changes in density and the thermal properties? This must be very important.

E. E. Agur. Such variations are important, but we have assumed constant values for the densities, thermal conductivities, and heat capacities in our model. Good predictions were obtained without the need for adjustable parameters or "fudge factors." The whole point of our model is that it is fully predictive. You are given the screw dimensions and the indicated resin properties, and the model yields a full process prediction.

Ch. I. Chung. The agreement between the measured values and the predictions, as far as extruder output is concerned, look quite good, but the pressure prediction is not. It is interesting to note that both the measured and predicted output values are virtually proportional to screw RPM. It seems that, since a small 1½ in. extruder has been used, substantial melting occurs, and there is not much of a pressure-flow effect. So what you are calculating and measuring is virtually drag flow. The situation may not be so favorable with a larger extruder. I tend to agree with Dr. Utracki that, with these crude assumptions, you are not going to have such a good fit.

E. E. Agur. I agree with you on this point. We have to look at, not only different sizes of extruders, but also different screw designs and different plastics.